Computers and Electronics in Agriculture 212 (2023) 108128

Contents lists available at ScienceDirect

Computers and Electronics in Agriculture

journal homepage: www.elsevier.com/locate/compag

An autonomous task assignment and decision-making method for coverage path planning of multiple pesticide spraying UAVs

Jing Huang [a,b], Yao Luo [c], Quan Quan [d], Ban Wang [e,*], Xianghong Xue [a], Youmin Zhang [f,*]

[a] Department of Automation and Information Engineering, Xi'an University of Technology, Xi'an, Shaanxi 710048, China
[b] Jiujiang Precision Measuring Technology Research Institute, Jiujiang, Jiangxi 332000, China
[c] AVIC Shenyang Aircraft Design & Research Institute, Shenyang, Liaoning 210100, China
[d] School of Automation Science and Electrical Engineering, Beihang University, Beijing 100191, China
[e] School of Aeronautics, Northwestern Polytechnical University, Xi'an, Shaanxi 710072, China
[f] Department of Mechanical, Industrial, and Aerospace Engineering, Concordia University, Montreal, Quebec H3G 1M8, Canada

ARTICLE INFO

Keywords:
Pesticide spraying
Task assignment
Coverage Path Planning (CPP)
Sequential Quadratic Programming (SQP)
Graphical User Interfaces (GUIs)
Stateflow
Pixhawk Autopilot

ABSTRACT

As the approaching of Agriculture 4.0 era and advancements of new technologies of Unmanned Aerial Vehicles (UAVs) and particularly quadcopter UAVs, plant protection quadcopters are becoming increasingly popular and practical in pesticide spraying, fertilization, pollination, seeding, and other agricultural activities. One of the main problems for plant protection quadcopters is completing planning tasks efficiently and quickly. Therefore, this paper proposes an autonomous task assignment and decision-making method for coverage path planning by multiple cooperative quadcopters. The Sequential Quadratic Programming (SQP) method is adopted to acquire the optimal solution for the proposed problem. Then, a simulation platform by MATLAB Graphical User Interfaces (GUIs) is established using the Stateflow technique, and multiple ZY-UAV-680 quadrotor UAVs are employed to carry out the actual flight tests. Finally, simulations and actual flight tests are conducted to demonstrate the effectiveness of the autonomous optimal task assignment and decision-making method. The final results show that: the proposed method can divide multiple UAVs reasonably to several blocks; the time differences between the simulation test and real flight test are only 39.8 sec and 20.6 sec, and accounts for 6.6% and 3.9% of the spraying time spent on real flight test by three cooperative quadrotors, respectively; the optimal scheme can save 60.8 sec and 80.0 sec in the simulation tests and the real flight tests, which accounts for 10.8% and 13.2% of the time spent on average scheme, respectively. Therefore, it can be concluded that the simulation results can match the real flight test results quite well regardless of average scheme or optimal scheme, and the optimal scheme is more efficient and timesaving than the average scheme.

1. Introduction

Recently, quadcopters have drawn significant attention in both military and civilian fields such as reconnaissance and strikes (Hassanalian and Abdelkefi, 2017; Zhou et al., 2020), forest fire monitoring (Hossain et al., 2019; Yuan et al., 2015), and precision agriculture (Mukherjee et al., 2019; Sinha, 2020), since they can work cooperatively in harsh or dangerous environments for human beings (Zuo et al., 2022). Agriculture 4.0 promotes conventional production methods and national agriculture strategies using state-of-the-art techniques, such as 5G communication, big data, cloud computing, Internet of Things (IoT), virtual reality, and so on. These techniques provide creative approaches at every step of the agricultural industry chain (Silveira et al., 2021; Yang et al., 2021). Especially in the field of precision agriculture, plant protection UAVs are being increasingly utilized in pesticide spraying, fertilization, seeding, agricultural insurance surveys, farmland information, and disease monitoring (Su et al., 2018; Sinha, 2020; Yang et al., 2021). The US, European countries and Canada have large farms for planting crops. In contrast, Asian countries like China, Japan, and South Korea concentrate on the plant protection UAV with a small capacity at a low altitude, considering that there are small complex terraces or mountains for planting crops (Wang et al., 2021; Xu et al., 2019). By 2019, the number of plant protection UAVs in China has exceeded 55,000 while the area planted by UAVs had also surpassed 566,667 km^2.

* Corresponding authors.
E-mail addresses: jinghuang411@icloud.com (J. Huang), luoyao920724@163.com (Y. Luo), qq_buaa@buaa.edu.cn (Q. Quan), wangban@nwpu.edu.cn (B. Wang), xhxue@xaut.edu.cn (X. Xue), youmin.zhang@concordia.ca (Y. Zhang).

https://doi.org/10.1016/j.compag.2023.108128
Received 30 March 2022; Received in revised form 29 July 2023; Accepted 3 August 2023

The traditional pesticide spraying method in the 1930s demands that a farmer should spray pesticides on crops manually with a knapsack sprayer. This method is prone to the following disadvantages:

(1) Through large-dose coarse droplet spraying, the utilization rate of pesticides is low with poor control effect;
(2) The sprayer needs to walk among the crops filled with atomized pesticides, and then his/her whole body is quickly soaked with pesticides, which always leads to severe poisoning.

As precision agriculture is developing fast, governments from different countries strongly encourage the development of UAVs to prevent and control pests or diseases in the local regions. Compared with traditional pesticide spraying methods by the knapsack sprayer, plant protection UAVs enjoy advantages such as high work efficiency, good maneuverability, small and uniform pesticide dosage per unit area, and the capability of vertical take-off and landing. Additionally, the remotely controlled plant protection UAVs can operate at a certain distance from the sprayed crops. This approach fundamentally solves the problem of operators being exposed to pesticide and helps avoid poisoning. Moreover, the vortex down-pressure atomized airflow produced by high-speed rotating blades can evenly spray pesticides on both the front and back sides of the crops' blades, which dramatically improves the spraying penetration rate and the effectiveness against pests and diseases (Li et al., 2022; Wang et al., 2021). Furthermore, several UAVs can implement a cooperative operation, which multiplies the spraying efficiency. In many aviation industry applications, the crucial issue of how to cover and traverse a specified area of interest has received particular attention from scholars and research institutes. This problem called Coverage Path Planning (CPP) is to determine an optimal flight path covering all points of a mission or Area of Interest (AOI) while avoiding obstacles (Macleod et al., 2018). In this paper, determining the deployment of multiple UAVs to realize pesticide spraying cooperatively is classified as a CPP problem. CPP primarily focuses on a variety of areas, such as search and coverage missions (Vinh et al., 2019), 5G network (Shi et al., 2020), 3D terrain reconstruction (Torres et al., 2016), sweep or area coverage (Macleod et al., 2018; Mansouri et al., 2018a, 2018b; Li et al., 2020; Glorieux et al., 2020), multiobjectives (Ellefsen et al., 2017), intracerebral hemorrhage evacuation (Granna et al., 2016), and especially modern agriculture (Yao et al., 2016; Du, 2017; Nilsson and Zhou, 2020; Sandamurthy and Ramanujam, 2020). More specifically, the applications in modern agriculture include arable farming (Nilsson and Zhou, 2020), harvesting in cashew orchards (Sandamurthy and Ramanujam, 2020), and precision spraying (Yao et al., 2016; Du, 2017). For different control objects, the CPP method is applied to underwater vehicles and gliders (Han et al., 2020; Sun et al., 2019), single robot (Galceran and Carreras, 2013; Nasr et al., 2019) or multi-robots (Galceran and Carreras, 2013; Nasr et al., 2019), and a single UAV (Torres et al., 2016; Dai et al., 2018) or multi-UAVs (Guastella et al., 2019). In general, almost all these similar path planning problems for multiple agents are regarded as NP-hard problems. In addition, the CPP method can be integrated with intelligent approaches to address specified problems, such as Mixed Integer Linear Programming (MILP) (Vinh et al., 2019), predator–prey (Hassan and Liu, 2020), bio-inspired neural network (Du, 2017), and ant-colony (Han et al., 2020).

For instance, Granna et al. (2016) established an optimized path from start to end using a map of the environment for the robot with an awareness of its location by the map. Sandamurthy and Ramanujam (2020) formulated a CPP algorithm for discrete harvest coverage in cashew orchards to solve the time-consuming and labor-intensive collection for fruits and nuts on the floor. By a novel Mahalanobis distance partitioning method, the algorithm can obtain an average coverage of 52.78% with only a deviation of 18.95%. Du (2017) proposed a hierarchical approach to deal with the allocation and path planning problem during a pesticide spraying mission in a hilly area via an inner-outer loop structure. The inner loop was modeled as a genetic algorithm-based Travelling Salesman Problem (TSP), while the outer loop utilized a nonlinear programming approach based on the optimal result from the inner loop. Hassan and Liu (2020) put forward an adaptive real-time predator–prey-based method to address the CPP problem with unexpected changes, which could tune the model parameters offline to minimize the path length. However, most existing papers considered the optimization issue as a continuous parameter model instead of a continuous integer planning one.

The papers above primarily focus on finding the optimal path with minimum distance to improve efficiency. Nevertheless, few of them have considered the constraints such as the limited power or fuel of vehicle. For illustration, in actual practice, quadcopters are only capable of working at a specific endurance and need to be charged or refueled repeatedly when the energy is running out. Li et al. (2020) identified this constraint problem. However, failing to focus on this problem in their work, they established a Min-Time Max Coverage (MTMC) sweep coverage model for cooperative UAVs to obtain the maximum high-quality coverage rate in minimum mission time simultaneously. Sundar and Rathinam (2014) abstracted this power limited CPP problem into Fuel Constrained, UAV Routing Problem (FCURP). Khuller et al. (2011) proposed an algorithm with an approximation factor for FCURP that fulfilled the triangle inequality with symmetric cost. Applying this algorithm to asymmetric cost, Sundar and Rathinam developed an approximation factor with two dependent constrained parameters, and construction/improvement heuristics to solve FCURP.

In this paper, we consider that the power or fuel is limited directly. When the power or fuel of the UAV is exhausted, it should return to the base to charge or refuel. Two major contributions can be outlined as follows:

(1) *Systematicness*: i) This paper proposes a comprehensive autonomous method for assigning tasks and decision-making for CPP problems using multiple cooperative quadcopters, including task assignment, path planning and traffic scheduling; ii) This paper develops an Extended Finite State Machine (EFSM) that defines seven modes and eight Automatic Trigger Events (ATEs) to describe eleven transformations;
(2) *Practicability*: i) Unlike previous studies (Lindner et al., 2019; Li et al., 2020), this paper considers the issue of limited power or fuel as a key constraint in practical applications of cooperative quadcopters for pesticide spraying; ii) This paper presents comparative flight tests using three ZY-UAV-680 quadcopter UAVs equipped with open-source Pixhawk autopilots.

This paper is organized as follows: in Section 2, the problem of pesticide spraying by cooperative quadcopters is formulated; in Section 3, the optimal location of the take-off point is demonstrated by the Pythagorean theorem; in Section 4, the mathematical model of pesticide spraying by cooperative quadcopters is established, and the SQP by the state machine is adopted to optimize the proposed problem; in Section 5, the air traffic scheduling system and the user's demands including the functional demand and safety demand are introduced to define the flight modes; and in Section 6 and Section 7, the simulation platform by MATLAB GUIs and Stateflow is established, and both the simulation and actual flight tests are conducted and testing results are analyzed.

2. Problem formulation

This section will formulate the problem of coverage path planning by multiple pesticide spraying UAVs. The general procedure of cooperative quadcopters' spraying mission is as follows: the quadcopter takes off vertically from the base to a specified altitude, and then flies to the block in a straight path and starts spraying. After all the spraying missions are finished, it returns to the base directly. The problem can be divided into three main points:

(1) How should multiple quadcopters be divided reasonably for several blocks? The dividing strategy should guarantee that the blocks either far away from the take-off point or with more spraying tasks should be allocated more quadcopters. Meanwhile, blocks either closer to the take-off point or with fewer spraying tasks should be assigned with fewer quadcopters. Eventually, each block approximately spends the same amount of time in completing the spraying task, and the whole time for the spraying mission will be minimized;
(2) Where should the quadcopters take off? The optimal strategy must decide the base position where the quadcopters should take off so that the charging/refueling time can be minimized in this base;
(3) How should an air traffic scheduling system be designed? The logical decision design should ensure that the cooperative quadcopters complete the pesticide spraying mission in the shortest time without any collision.

Fig. 1 depicts the assignment performing scheme by cooperative quadcopters. Several blocks in different shapes are on both sides of the broken line ridge road. The shape of the blocks can be regular or irregular. Several quadcopters take off from the take-off points to implement the pesticide spraying tasks. The following section will focus on the three parts: optimal location of the take-off point, optimal path planning, and air traffic scheduling. Fig. 2 depicts the schematic diagram of a rectangular task in which four quadcopters are employed to carry out the pesticide spraying task, where l_i and w_i denote the length and width of the ith block, and w_0 denotes the pesticide spraying width of quadcopters. When the length and width of the block are inputted into the designed MATLAB GUI App, it will calculate the data of the block, and generate the spraying path automatically by Boustrophedon method (Choset and Pignon, 1998). As shown in Fig. 2, similar as an ox drags a plow in a field, the quadrotor moves in a straight line across the full length of the block, turns around, and follows a new straight-line path parallel to the previous one. By repeating this procedure, the quadrotor can cover the entire block. The width of adjacent parallel paths is equal to the pesticide spraying width of quadcopters w_0.

The goal of the allocation strategy is to determine the base position and the number of quadcopters corresponding to each block based on the known starting and ending positions of the road, the total number of quadcopters, and the sizes and locations of the blocks. The allocation principle is to assign more quadcopters to the block far away from the base or the larger block with more spraying tasks. Meanwhile, fewer quadcopters should be allocated to the block close to the base or the smaller block with fewer spraying tasks. The final goal is to ensure that the time spent on the spraying task of each block is roughly the same, so the time spent on the whole spraying task will be minimized. To facilitate the mathematical modeling process, we make the following assumptions for the allocating and scheduling issues:

(1) The quadcopters can only take off from the ridge road. If a vertical line is drawn from the center of the block to the centerline of the road, the vertical foot will be the take-off point for the quadcopter;
(2) The number of quadcopters used to spray pesticides for one block should not be smaller than one, and one quadcopter is only responsible for the task of one block;
(3) The quadcopters which conduct pesticide spraying tasks of the same block should take off from the identical take-off point of this block.

3. Optimal location of take-off point

This section will demonstrate the position rationality of the take-off point's position to ensure the strictness of the mathematical model. Fig. 3 depicts the block, road, and base position scheme for the quadcopters, where point $\boldsymbol{p}_0$ is the central point of the block, and points $\boldsymbol{p}_1$ and $\boldsymbol{p}_2$ are two different take-off points, respectively. Point $\boldsymbol{p}_1$ should meet the condition that straight-line $\boldsymbol{p}_0\boldsymbol{p}_1$ is perpendicular to the centerline of ridge road $\boldsymbol{p}_1\boldsymbol{p}_2$. $d_{k,1}$ and $d_{k,2}$ represent the distances between the central point of the block $\boldsymbol{p}_0$ and take-off point $\boldsymbol{p}_1$ and take-off point $\boldsymbol{p}_2$, respectively. It is obvious that the perpendicular distance from a point to a line is the shortest by the Pythagorean theorem, so it is concluded that $d_{k,1} < d_{k,2}$.

4. Optimal path planning

This section will introduce the optimal path planning process. Fig. 4. depicts the scheme of the different flight paths for cooperative quadcopters. In Fig. 4, $\boldsymbol{p}_{f,i}$ is the coordinates of take-off point, i.e., the base, and $\boldsymbol{p}_i$ is the central point's coordinates of the ith block. The total flight path of the kth quadcopter includes four kinds of lines: the two-dot dashed purple line depicts the path $p_{k,1}$ through which the quadcopter begins pesticide spraying and Returns To Base (RTB) after all the tasks are finished, the dashed green line depicts the regular pesticide spraying path $p_{k,2}$, the solid black line depicts the switching path $p_{k,3}$ between

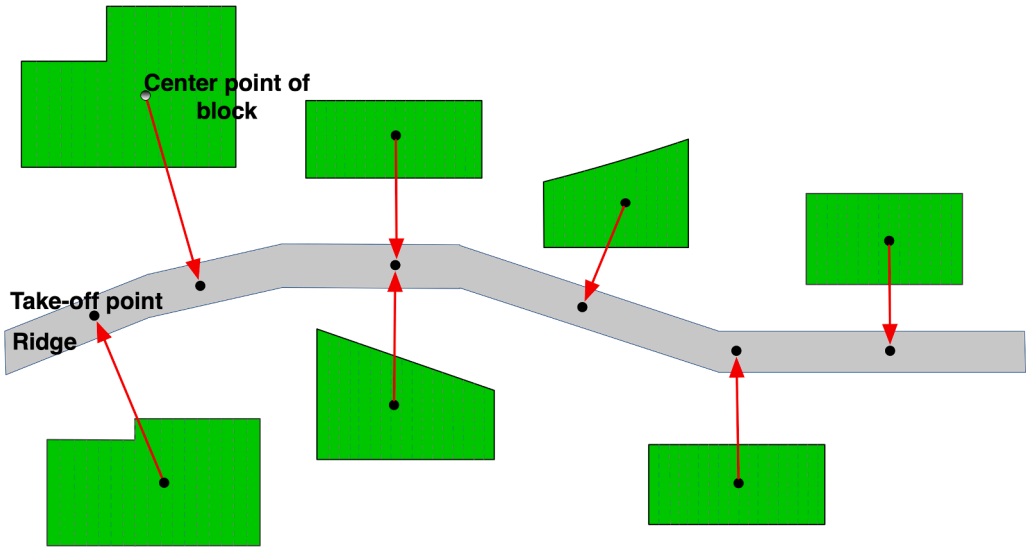

Fig. 1. The assignment performing scheme by cooperative quadcopters.

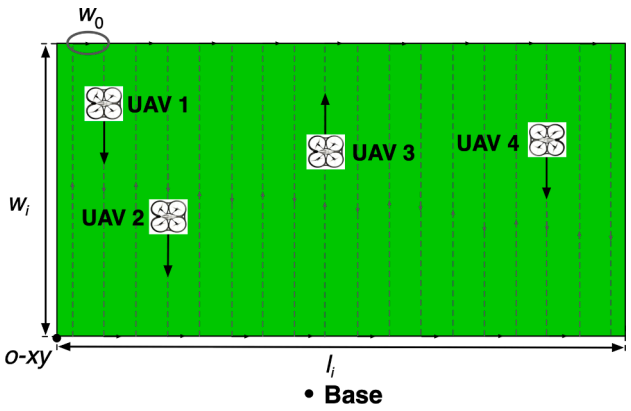

Fig. 2. The schematic diagram of a rectangular task.

two-unit spraying tasks, the dot-dashed red line depicts the RTB charging or refueling path $p_{k,4}$, and d_k denotes the distance between the center of the task assigned to the kth quadcopter and the base.

The following assumptions are proposed to simplify the problem and establish a mathematical model for the task:

(1) Each quadcopter has the identical charging or refueling distance. Taking the kth quadcopter for example, the RTB charging or refueling path $p_{k,4}$ differs each time, and different task allocation strategies will lead to varied numbers of spraying paths n_k and different returning paths $p_{k,1}$ at the end of the spraying task. However, to simplify the problem and establish a reasonable mathematical model, the distance between the center of the task assigned to the kth quadcopter and the base point d_k is supposed to be a round-trip constant distance approximately. The distance between the center point of the quadcopter's mission and the base is defined as the constant distance for each charging or refueling process;

(2) The location and area of the block are given, but the shape of the block can be rectangle, square and trapezoid;

(3) In general, it is assumed that the speed of the quadcopter is identical, and the acceleration and deceleration processes during taking-off, cruising, spraying, and landing are neglected;

(4) All the quadcopters have almost the same maximum power or fuel and the same charging or refueling time by ignoring subtle differences among individuals. This is because if the maximum power or fuel and the charging or refueling time of each quadcopter are different, the mathematical model will be too complicated to establish. Therefore, to facilitate the establishment of the mathematical model, we assume that all the quadcopters are of the same type.

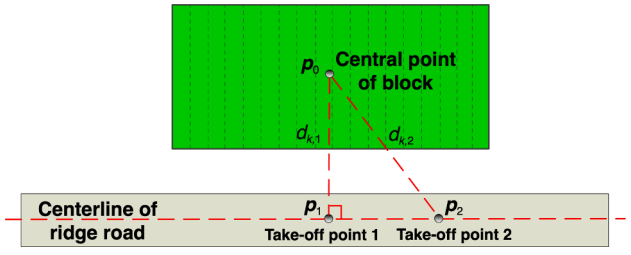

Fig. 3. The block, road, and base position scheme for the quadcopters.

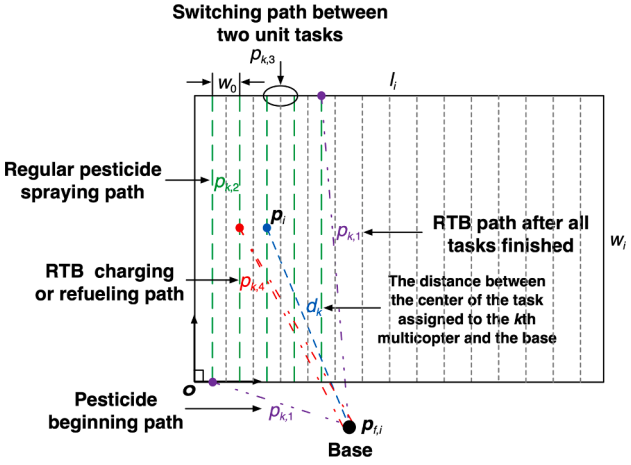

Fig. 4. The scheme of the different flight paths for cooperative quadcopters.

A total number of m quadcopters are allocated for the whole pesticide spraying task. The block can be divided into equal intervals, and its total number n can be obtained as follows:

$$n = \frac{l_i}{w_0} \tag{1}$$

The sum of tasks $\overline{n}_{k-1}$ assigned to the total previous $(k-1)$ quadcopters is given as follows:

$$\overline{n}_{k-1} = \sum_{i=1}^{k-1} n_i \tag{2}$$

where n_i is the number of spraying paths by the ith quadcopter. Furthermore, the total number of spraying paths by all quadrotors can be written as follows:

$$n = \sum_{i=1}^{m} n_i \tag{3}$$

The distance between the center of the task assigned to the kth quadcopter and the base can be obtained by the following equation:

$$d_k = \sqrt{\left(p_{i,x} - p_{f,i,x}\right)^2 + \left(p_{i,y} - p_{f,i,y}\right)^2} \tag{4}$$

where $\left(p_{i,x}, p_{i,y}\right)$ and $\left(p_{f,i,x}, p_{f,i,y}\right)$ are the coordinates of $\boldsymbol{p}_i$ and $\boldsymbol{p}_{f,i}$. Suppose that k_{line} is the slope of the ridge road straight-line equation as follows:

$$k_{line} = \frac{p_{s,y} - p_{e,y}}{p_{s,x} - p_{e,x}} \tag{5}$$

where $\boldsymbol{p}_s$ and $\boldsymbol{p}_e$ are the starting and ending points of the ridge road, respectively. $\left(p_{s,x}, p_{s,y}\right)$ and $\left(p_{e,x}, p_{e,y}\right)$ are the coordinates of $\boldsymbol{p}_s$ and $\boldsymbol{p}_e$, respectively.

The intercept of the centerline of the ridge road equation can be obtained as follows:

$$b = p_{e,y} - k_{line} p_{e,x} \tag{6}$$

The take-off point of the quadcopter should be on the centerline of the ridge road:

$$p_{f,i,y} = k_{line}\ p_{f,i,x} + b \tag{7}$$

The straight-line $\boldsymbol{p}_i\boldsymbol{p}_{f,i}$ is perpendicular to the centerline of the ridge road $\boldsymbol{p}_s\boldsymbol{p}_e$:

$$\frac{p_{i,y} - p_{f,i,y}}{p_{i,x} - p_{f,i,x}} \cdot \frac{p_{s,y} - p_{e,y}}{p_{s,x} - p_{e,x}} = -1 \tag{8}$$

So, the constraints on the take-off point, the central point of the block, and the ridge road centerline are provided as follows:

$$\left(p_{i,x} - p_{f,i,x}\right)\left(p_{s,x} - p_{e,x}\right) + \left(p_{i,y} - p_{f,i,y}\right)\left(p_{s,y} - p_{e,y}\right) = 0 \tag{9}$$

The distance between the center of the task assigned to the kth quadcopter and the base can be rewritten as follows:

$$d_k = \sqrt{w_0^2\left(\frac{n}{2} - \sum_{i=1}^{k-1} n_i - \frac{n_k}{2}\right)^2 + \left(\frac{w_r}{2}\right)^2}$$

$$= \sqrt{w_0^2\left(n/2 - \overline{n}_{k-1} - n_k/2\right)^2 + \left(w_r/2\right)^2} \tag{10}$$

To simplify the modeling process, the starting and ending flight path length $p_{k,1}$ is supposed to be approximately double d_k as follows:

$$p_{k,1} \approx 2d_k \tag{11}$$

The regular pesticide spraying path $p_{k,2}$ is given by the following expression:

$$p_{k,2} = n_k w_r \tag{12}$$

where n_k is the number of spraying paths by the kth quadcopter. The switching path $p_{k,3}$ between two-unit tasks can be calculated by the following expression:

$$p_{k,3} = (n_k - 1)w_0 \tag{13}$$

Similarly, the length of RTB charging/refueling flight path is also assumed to be approximately equal to d_k, so the total RTB charging or refueling path can be derived as follows:

$$p_{k,4} \approx 2n_{k,c}d_k \tag{14}$$

where $n_{k,c}$ is the charging/refueling times of the kth quadcopter. Therefore, the whole pesticide spraying time spent on completing spraying tasks includes four parts as follows:

$$t_{k,i} = \frac{p_{k,i}}{V}, i = 1, \cdots, 4 \tag{15}$$

where $p_{k,i}$ is the ith flight relevant path of the kth quadcopter, and V is the average speed of all the quadcopters, which is assumed to be a constant. Then, the total time spent by the kth quadcopter t_k is calculated by the following equation:

$$t_k = \frac{\sum_{i=1}^{4} p_{k,i}}{V} + n_{k,c}T_c$$

$$\approx \frac{n_k w_r + (n_k - 1)w_0 + 2\left(n_{k,c} + 1\right)d_k}{V} + n_{k,c}T_c \tag{16}$$

where T_c is the RTB charging/refueling time.

It is supposed that the kth quadcopter is fully charged/refueled when starting the pesticide spraying mission, and it is almost exhausted when flying back to the base. To guarantee that the quadcopter still has enough power/fuel to fly back to the take-off point after finishing pestiside spraying, it is ensured that the total length of the flight path should not only be larger than the charging/refueling flight distance for $n_{k,c}$ times, but also be smaller than or equal to the charging/refueling flight distance for $\left(n_{k,c} + 1\right)$ times. The constraints above can be expressed by a group of inequalities as below:

$$\begin{cases} p_{k,1} + p_{k,2} + p_{k,3} + p_{k,4} > V n_{k,c} T_b \\ p_{k,1} + p_{k,2} + p_{k,3} + p_{k,4} \le V\left(n_{k,c} + 1\right)T_b \end{cases} \tag{17}$$

where T_b is the flight time of each quadcopter after fully charging/refueling. Therefore, the optimized objective function of the quadcopters' allocating and scheduling problem in this paper can be given as follows:

$$\min_{n_k, n_c \in \mathbb{Z}+} \sum_{i=1}^{m} \left(t_i - \frac{\sum_{i=1}^{m} t_i}{m} \right) \tag{18}$$

More specifically, to minimize the maximum working time of the multiple quadcopters, all quadcopters should complete the spraying mission and return to the base at the same time as possible. The detail of the objective function is summarized in **Algorithm 1** below.

Algorithm 1 Objective optimization function

```
/* Initialization */
Initialize the number of quadcopters m;
Initialize the time expectation and variance of spraying task by m quadcopters [(∑_{i=1}^{m} t_i)/m, σ^2];
/* Main function */
for i = 0 to m do
    Sum up the time spent on spraying task by m quadcopters ∑_{i=1}^{m} t_i;
end
Calculate the expectation of spraying task by m quadcopters (∑_{i=1}^{m} t_i)/m;
for j = 1 to m do
    Calculate the variance of sprayed task by m quadcopters σ^2;
end
```

Based on (2), (3), (10), (16), and (17), the optimization objective (18) should be subject to a group of constraints as follows:

$$t_k \approx \frac{n_k w_r + (n_k - 1)w_0 + 2\left(n_{k,c} + 1\right)d_k}{V} + n_{k,c}T_c \tag{19a}$$

$$n_k w_r + (n_k - 1)w_0 + 2\left(n_{k,c} + 1\right)d_k > V n_{k,c} T_b \tag{19b}$$

$$n_k w_r + (n_k - 1)w_0 + 2\left(n_{k,c} + 1\right)d_k \leqslant V\left(n_{k,c} + 1\right)T_b \tag{19c}$$

$$d_k = \sqrt{w_0^2\left(\overline{n}_{k_0} + n_m/2 - n/2\right)^2 + \left(w_r/2\right)^2} \tag{19d}$$

$$\overline{n}_{k-1} = \sum_{i=1}^{k-1} n_i \tag{19e}$$

$$n = \sum_{i=1}^{m} n_i \tag{19f}$$

The details of nonlinear constraints are summarized in **Algorithm 2** as follows:

(1) Eq. (19a) represents the time to complete the spraying missions of the kth quadcopter, which is equal to the total sum of the flight paths divided by the average speed of quadcopter plus the total charging/refueling time thereafter;
(2) Eqs. (19b) and (19c) are the flight distance constraints. More specifically, the total flight distance of the kth quadcopter to complete the missions should not be smaller than or equal to the distance when it can fly $\left(n_{k,c} + 1\right)$ times. Meanwhile, it should be larger than the distance when it can fly $n_{k,c}$ times after fully charging/refueling each time. These two proposed inequalities ensure that the energy of the quadcopter is almost exhausted when it flies back to the base;
(3) Eq. (19d) represents the evaluated round-trip distance between the base and the block. To simplify the model establishment, both the starting or ending flight path length $p_{k,1}$ and the charging/refueling flight path $p_{k,4}$ are approximately equal to the distance between the center of the task of kth quadcopter and the base d_k;
(4) Eq. (19e) defines $\overline{n}_{k-1}$ as the sum of missions allocated to the total previous $(k-1)$ quadcopters, which is utilized to calculate the constant distance d_k;
(5) Eq. (19f) defines n as the sum of the number of missions allocated to m quadcopters.

Algorithm 2 Nonlinear constraints function

```
/* Initialization */
Initialize the number, the spraying width, the charging/refueling time, and the maximum flight time of quadcopters [m, w_0, T_c, T_b];
/* Main function */
for k = 1 to n do
Set up the starting and ending points of spraying paths on the field;
end
for i = 1 to m do
Sum up the spraying paths number of the front (k − 1) quadcopters by Eq. (19e);
Sum up the spraying paths number of all the quadcopters by Eq. (19f);
Sum up the length of front i spraying paths ∑_{i=1}^{m} H_i;
End
for i = 1 to m do
Calculate the time spent on spraying mission of each quadcopter by Eq. (19a);
Calculate flight distance constraint by Eqs. (19b) and (19c);
Calculate the round-trip distance by Eq. (19d);
end
```

5. Air traffic scheduling

This section will elucidate the general pesticide spraying process of multiple quadcopters on the blocks. First, the quadcopters take off vertically from the base to a specified altitude. Then, they fly straight to the sprayed block. Afterwards, they reach the corresponding blocks and start the spraying missions. Finally, after all the spraying mission is completed, they fly back to the base in a straight path.

5.1. Priority level

Since the behavior of the controlled object should meet all the user's demands, the design process of an air traffic scheduling system should include the following four steps:

(1) Propose the functional and safety demands on the quadcopter based on actual problems;
(2) Define the modes and events of the quadcopter according to the functional and safety demands;
(3) Use the proposed functional demands and events of the quadcopter to generate an automaton, and then adopt the automaton as the controlling demand;
(4) Use the controlled object and controlling demands to generate an EFSM controller.

5.2. User demands

The user's demands fall into two categories: functional demands and safety demands. Both of them will be described in detail.

5.2.1. Functional demands

As illustrated below, there are five functional demands during the flight of quadcopter.

(1) It will arm according to the demands, and then take off;
(2) After it takes off, it can automatically switch between different modes according to the demands;
(3) It can land automatically or return to the take-off point according to the demands, and disarm itself;
(4) The starting and ending of the spraying process can be controlled according to the demands;
(5) It can realize the altitude hold mode and the loiter mode.

5.2.2. Safety demands

The collisions of UAVs possibly take place when they take off or land. Given that the UAVs are separated in different parts of a block during a spraying or non-spraying flight path, there is no risk of collision during the spraying operations. Before enumerating the safety demands, it is necessary to define the safety distance thresholds and priorities of different quadcopters. The safety distance thresholds are determined by the size and flight characteristics of the quadcopters. The priorities of the quadcopters are directly related to the mode they are in. Once the distances of the quadcopters are smaller than the safe distance during the flight, the corresponding anti-collision strategies will be adopted according to different priorities. The safety demands on the pesticide spraying system are given as follows:

(1) When the quadcopters are landing at the same base point, the quadcopters that are preparing to land should hover and wait, and the others on the ground should postpone the take-off process simultaneously;
(2) When the quadcopters are taking off at the same take-off point, the quadcopters that are preparing to land should hover and wait, while the others on the ground should postpone the take-off process;
(3) If quadcopter A with a higher priority is prone to collide with quadcopter B, that is, if the distance between each other is within the safety threshold, quadcopter A keeps flying straight, while quadcopter B should avoid collision. During the avoidance process, quadcopter B should always maintain a sufficiently safe distance from quadcopter A and try to move along the previous straight path to the target point. If quadcopter A with the same priority is prone to collide with quadcopter B, quadcopter A and B should avoid collision simultaneously. During the avoidance process, they always keep a sufficiently safe distance from each other, and thereafter they try to move along the previous straight path to the target point. If quadcopter A with a lower priority is prone to collide with quadcopter B, quadcopter A should avoid collision while quadcopter B keeps flying straight. During the avoidance process, quadcopter A should always keep a sufficiently safe distance from quadcopter B and thereafter try to move along the previous straight path towards the target point;
(4) When several quadcopters are in danger of collisions at the same time, quadcopter A with a higher priority will keep flying in a straight line while the others should avoid collision and maintain a sufficient safe distance from each other if it has a higher priority than the others. After that, the others should try to move along the previous straight paths to the target points, respectively. If quadcopter A has the same priority as the others, all of them should avoid collision and always keep a sufficiently safe distance from each other. Afterwards, they should try to follow the previous straight line to the target points, respectively;
(5) After the avoidance process is completed, the corresponding quadcopter will continue to follow its original flight path or work;
(6) When a flying quadcopter fails, it will return to the base or land automatically and immediately.

5.2.3. Flight Mode definition

The whole spraying process of the quadcopter from take-off to landing is divided into seven different flight modes as follows:

(1) *Standby Mode*: The quadcopter will immediately enter this mode when the power module is powered on;
(2) *Take-off Mode*: The quadcopter will immediately enter this mode when it receives a take-off command in the standby mode, and it will take off vertically from the base point until it reaches the specified altitude;
(3) *Onway Mode*: In this mode, the quadcopter takes a round trip between the block and the take-off point, which includes two parts: the state when the quadcopter flies from the base point to the block after taking off, and the state when it flies back to the take-off point overhead before landing;

(4) *Work Mode*: In this mode, the quadcopter sprays pesticides on the block after reaching the block;
(5) *Land Mode*: The quadcopter will immediately enter this mode when it returns to the take-off point and lands vertically;
(6) *Rest Mode*: The quadcopter will immediately enter this mode after it lands at the take-off point and take a rest;
(7) *Disabled Mode*: In this mode, the quadcopter is disabled.

5.2.4. Extended Finite state Machine

Eight Automatic Trigger Events (*ATEs*) and three priorities by MATLAB Stateflow are developed for cooperative quadrotors to avoid collisions during the flight between the bases and the block. *ATEs* describe the mode transitional conditions. *ATEs* are independent of the remote pilot's operations and primarily produced by the current status of the quadcopter and its components (Quan, 2017; Quan et al., 2020). Eight different couples of *ATEs* are defined in Table 1. Based on the flight modes and *ATEs* of the quadcopters, the flight logic for the quadcopters is designed as an EFSM, as shown in Fig. 5, where C$i, i = 1, \cdots, 11$ represents the transitional condition. The transitional conditions are illustrated as follows:

C1: (ATE 2 == 0) & (ATE 4 == 0) & (ATE 5 == 0)

This condition indicates that the quadcopter keeps *Work Mode*. It implies that 1) its spraying task has not been finished (ATE 2 == 0); 2) the next waypoint is not the pesticide spraying working waypoint (ATE 4 == 0); and 3) it has not reached the target point (ATE 5 == 0).

C2: [(ATE 2 == 1) & (ATE 5 == 1)] | (ATE 4 == 0)

This condition implies a switch from *Work Mode* to *Onway Mode*. Such a switch can take place in one of the following two cases: 1) the spraying task has been finished (ATE 2 == 1) while the quadcopter has reached the target point (ATE 5 == 1); or 2) the next waypoint is not the pesticide spraying working waypoint (ATE 4 == 0).

C3: (ATE 2 == 0) & (ATE 4 == 1) & (ATE 5 == 1)

This condition implies a switch from *Onway Mode* to *Work Mode*. This switch requires the three following cases to hold simultaneously: 1) the quadcopter has not finished the spraying task (ATE 2 == 0); 2) the next waypoint is the spraying working waypoint (ATE 4 == 1); and 3) it has reached the target point (ATE 5 == 1).

C4: [(ATE 2 == 1) & (ATE 5 == 1)] | (ATE 4 == 0)

This condition indicates that the quadcopter remains in *Onway Mode*, including one of the following two cases: 1) the quadcopter has finished the spraying mission (ATE 2 == 1) while it has reached the target point (ATE 5 == 1) or 2) the next waypoint is not the pesticide spraying working waypoint (ATE 4 == 0).

C5: (ATE 5 == 1) & (ATE 6 == 1)

Table 1
The description of Automatic Trigger Events.

Event	Description
ATE 1	Charging or refueling status of the quadcopter (1: fully; 0: not fully).
ATE 2	Working status to finish the pesticide spraying mission (1: has; 0: has not).
ATE 3	Taking-off status to reach the specified altitude (1: has; 0: has not).
ATE 4	Working status of the next waypoint to spray pesticide (1: is; 0: is not).
ATE 5	Working status to reach the target point (1: has; 0: has not).
ATE 6	Onway status to arrive over the takeoff point (1: has; 0: has not).
ATE 7	Landing status to reach the base point (1: has; 0: has not).
ATE 8	Fault status of the quadcopter (1: fault; 2: faultless).

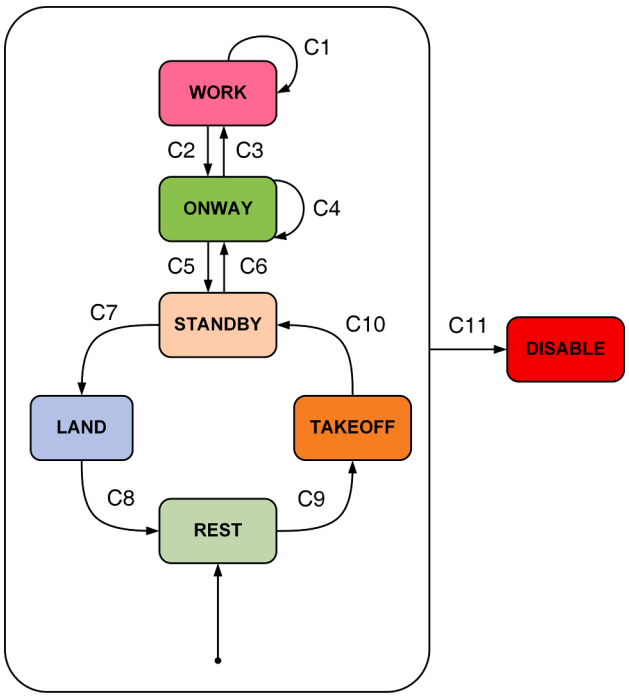

Fig. 5. The EFSM of cooperative quadcopters for spraying pesticides.

This condition implies a switch from *Standby Mode* to *Onway Mode*. Such a switch will be triggered when the following conditions hold at the same time: 1) the quadcopter has reached the target point (ATE 5 == 1); and 2) it has arrived over the take-off point (ATE 6 == 1).

C6: (ATE 2 == 0) & (ATE 4 == 1)

This condition implies a switch from *Onway Mode* to *Standby Mode*. It implies that 1) the quadcopter has not finished the pesticide spraying mission (ATE 2 == 0); and 2) the next waypoint is the working waypoint for spraying pesticides (ATE 4 == 1).

C7: (ATE 2 == 1) | (ATE 4 == 0)

This condition indicates a switch from *Standby Mode* to *Land Mode* when 1) the quadcopter has finished the pesticide spraying task (ATE 2 == 1); or 2) the next waypoint is not the working waypoint for spraying pesticides (ATE 4 == 0).

C8: ATE 7 == 1

This condition indicates a switch from *Land Mode* to *Rest Mode* when the quadcopter has reached the base point.

C9: (ATE 1 == 1) & (ATE 2 == 0)

This condition implies a switch from *Rest Mode* to *Take-off Mode* when 1) the quadcopter is fully charged/refueled (ATE 1 == 1); and 2) it has not finished the spraying mission (ATE 2 == 0).

C10: (ATE 3 == 1) & (ATE 4 == 1)

This condition describes a switch from *Take-off Mode* to *Standby Mode*. It is required that 1) the quadcopter has reached the specified altitude (ATE 3 == 1); and 2) the next waypoint is the working waypoint for spraying pesticides (ATE 4 == 1).

C11: ATE 8 == 1

This condition indicates that the flight mode switches to *Disabled Mode* when the quadcopter suffers from a fault in the mode other than disabled mode ($ATE\ 8 == 1$).

6. Simulation and real flight tests

In this section, both the simulation tests and real flight test are carried out to verify the rationality and validity of the proposed optimal task allocation scheme.

6.1. Simulation tests

A MATLAB GUIs-based simulation platform is established for pesticide spraying by cooperative quadcopters. Then, the comparative simulation tests by optimal and average task allocation schemes are conducted in the established platform.

6.1.1. Simulation platform

Fig. 6. depicts the simulation platform scheme of quadcopters' cooperative spraying pesticides for the field. As shown in Fig. 6, the user can input parameters and display simulation results by the designed GUI as a human–computer interface. Specifically, the user provides the basic parameters, such as the location of the base point and the current point, the location and size of the block, the quadcopters states, the maximum electric quantity, the charging rate, and the consuming rate for initialization.

The simulation platform primarily includes three modules: a mission assignment module in brown, a path generating module in magenta, and a status determination module in yellow. More specifically, the mission assignment module conducts the optimal mission assignment scheme, the waypoints generation, and the path planning scheme based on the proposed parameters. The path generating module provides the flight path of each quadcopter to complete the pesticide spraying task according to the position of its take-off point, the position and size of the block, and the task allocation scheme. The status determination module displays the process of spraying pesticides on the block in real time based on the provided data on the simulation platform, and it determines the current state of the quadcopter according to its real-time flight path points. The current state of the quadcopter will be displayed in the quadcopter status bar of the simulation platform, including status, altitude, speed, and other information.

As shown in Fig. 6, to control the simulation progress and facilitate the display of the simulation results, a simulation control zone is designed in the simulation platform, which contains four control buttons: "Deploy!", "Pause/Continue", "Stop", and "Close". The user can click on "Deploy!" to start the simulation experiment, "Pause" to suspend the simulation, "Continue" to resume the simulation, "Stop" to end the simulation, and "Close" to shut the GUIs interface, respectively.

6.1.2. Simulation tests

The simulation experiments are conducted on a computer with an Intel Core i7-10510U CPU, 16.0 GB RAM, NVIDIA GeForce MX250 Display Adapter by Windows 10.

(1) Task Assignment Test

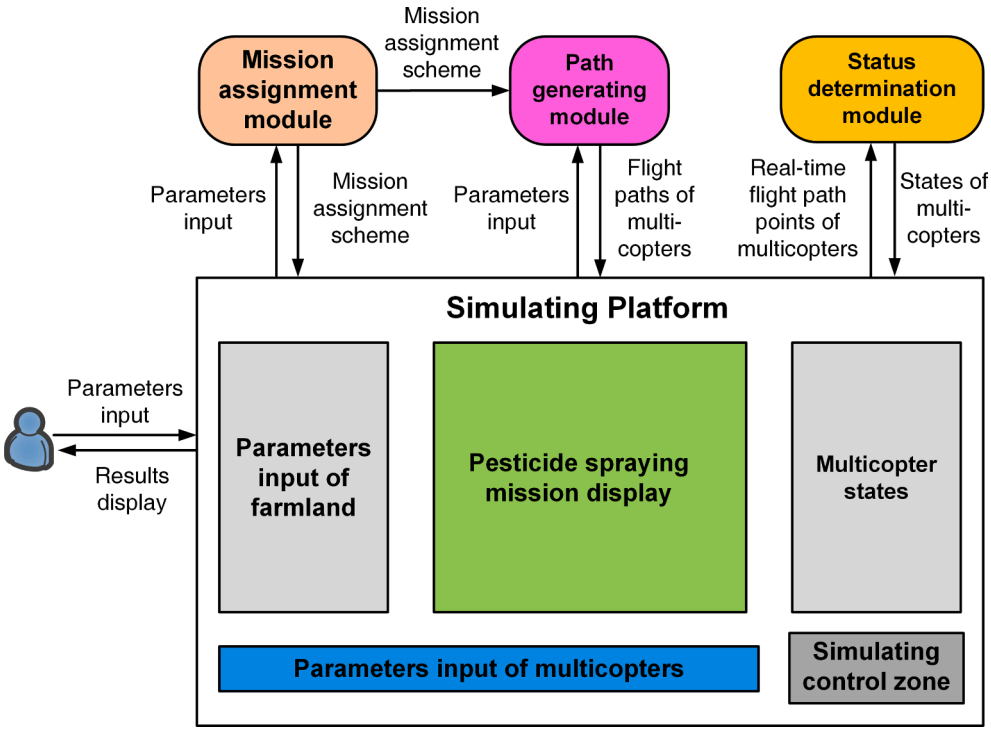

Fig. 6. The simulation platform scheme of quadcopters' cooperative spraying pesticides for the field.

Table 2
The block parameters of six blocks with different sizes and positions.

Test scheme	Block 1	Block 2	Block 3	Block 4	Block 5	Block 6
p_i	(500, 400)	(1500, 100)	(2500, 200)	(1000, −400)	(2000, −200)	(3000, −100)
D_i	400	100	200	400	200	100
N_i	80	40	80	40	40	80
h_i	100	100	100	100	100	100

When the quadrotors spray pesticides, the width w_0, speed V, charging time T_c and endurance after each charge T_b are 10 m, 5 m/s, 50 s and 400 s, respectively. The coordinates of the road starting point $\boldsymbol{p}_s$ and ending point $\boldsymbol{p}_e$ are (0, 0) and (5000, 0) respectively, the number of available quadrotors n is 20, and the number of spraying blocks m is 6. The information of the fields to be sprayed is shown in Table 2. Judging from the center point $\boldsymbol{p}_i$ and the approximate round-trip charging distance D_i of ith block, it can be seen that Block 1 and Block 4 are far away from the road, Block 2 and Block 6 are closest to the road, and Block 3 and Block 5 are centered from the road. When considering the number of spraying paths N_i and the length h_i of each spraying path in the block, it is shown that Block 1, Block 3 and Block 6 are larger, while Block 2, Block 4 and Block 5 are smaller. Combining all the above information, it can be inferred that Block 1 is a larger field in a farther location, Block 2 is a smaller field in a closer location, Block 3 is a larger field in a center location, Block 4 is a smaller field in a farther location, Block 5 is a smaller field in a central location, and Block 6 is a larger field in a closer location. In this example, it is assumed that all the blocks are regular rectangular farmlands, and all the roads are straight roads. However, in the actual situation, there may be irregularities in both fields and roads. So, if we want to use the above algorithm to find the optimal allocation scheme for the quadrotors, firstly, the blocks are approximated as a regular polygon, geometric knowledge is utilized to find the center point of each block, and then the roads are approximated as broken lines to be solved according to the straight road. To visualize the problem, the relative positions of the blocks and the roads are shown in Fig. 7.

The purpose of allocating multiple quadrotors is to assign more quadrotors to blocks that are far from the take-off point with more spraying tasks, but fewer quadrotors to blocks that are closer to the take-off point with fewer spraying tasks. Therefore, each field costs approximately the same amount of time to complete pesticide spraying. According to the allocation algorithm of quadrotors, it is apparent that in Fig. 7, Block 1 should be allocated the maximum number of quadrotors, while Block 2 should be allocated the minimum number of quadrotors. For example, Block 1 and Block 4 have the same distance to the straight road, but Block 1 is larger than Block 4, so Block 1 should be allocated more quadcopters than Block 4. Similarly, Block 6 should be allocated more quadcopters than Block 2, and Block 3 should be allocated more quadcopters than Block 5. When blocks are of the same size, a field farther from a straight road should be allocated more quadcopters than a farmland closer to a straight road. For instance, Block 1, Block 3 and Block 6 are of the same size, but Block 1 is farther away from the road, Block 3 is moderate away from the road, and Block 6 is closer to the road. Accordingly, the number of quadcopters allocated to these three Blocks can be arranged in descending order: Block 1, Block 3 and Block 6. Likewise, the number of quadcopters assigned to other three blocks can be arranged in descending order are: Block 4, Block 5 and Block 2.

Table 3
The allocation optimization results of quadrotors allocated to different blocks.

Allocating scheme	Block 1	Block 2	Block 3	Block 4	Block 5	Block 6
Allocating results	5.4881	1.8812	4.0698	2.8725	2.0707	3.6178
Rounding results	5	2	4	3	2	4

As listed in Table 3, for the scenario shown in Fig. 7, the number of quadcopters allocated to Block 1 to Block 6 is 5, 2, 4, 3, 2, and 4, respectively. It is also found that the numbers of quadcopters assigned to the three larger fields are: Block 1, Block 3 and Block 6 in descending order, while the numbers of quadcopters assigned to the three smaller fields are: Block 4, Block 5 and Block 2 in descending order. Although both Block 2 and Block 5 should be allocated two quadrotors after the optimization result is rounded, the number of quadrotors allocated to Block 2 is indeed smaller than that of Block 5 before it is not rounded. Therefore, the above statement is reasonable. In summary, it can be concluded that the algorithm proposed in this paper can reasonably allocate quadrotors, and its optimization results are reasonable and

Table 4
The initialization priority parameters of multiple quadcopters.

Serial number	Take-off point location	Target point location	Priority
1	(0, 62, 0)	(300, 362, 50)	1
2	(300, 62, 0)	(0, 362, 50)	2
3	(150, 0, 0)	(150, 497, 50)	3
4	(0, 0, 0)	(350, 350, 50)	1
5	(250, 0, 0)	(250, 448, 50)	2
6	(0, 250, 0)	(450, 250, 50)	3
7	(200, 0, 0)	(200, 430, 50)	1
8	(300, 30, 0)	(100, 430, 50)	2
9	(0, 330, 0)	(400, 130, 50)	3
10	(100, 0, 0)	(200, 500, 50)	1
11	(0, 100, 0)	(500, 200, 50)	2
12	(0, 200, 0)	(350, 200, 50)	1
13	(70, 0, 0)	(20, 400, 50)	2
14	(330, 0, 0)	(330, 400, 50)	3

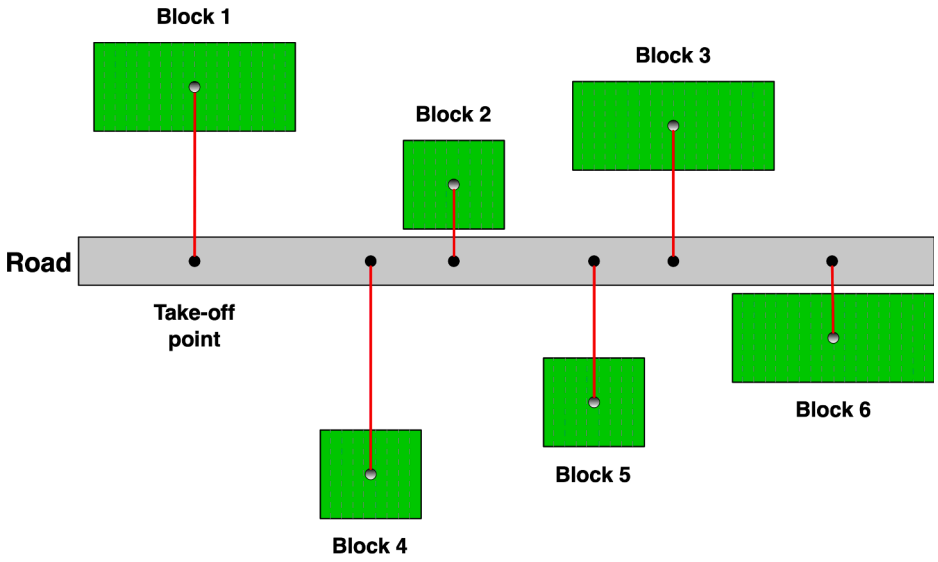

Fig. 7. The relative position scheme of field and road.

correct.

(2) Collision Avoidance Test

In the collision avoidance test, a total of 14 quadrotors were used, and their take-off points, target positions, and priorities listed in Table 4. The positions of the take-off and target points are composed of x, y, and z coordinates, and the target points are the geometric centers of the block. This is because in the collision avoidance test of multiple quadcopters, our primary concern is the flight safety of the quadcopters when flying back and forth from the take-off point to the block, and the quadcopters are less likely to collide with each other when spraying pesticides on the block. To achieve the desired results, the priorities of the 14 quadcopters were initialized with three different values, ranging from low to high: 1, 2, and 3.

Fig. 8 depicts the collision avoidance for multiple quadrotors from the take-off point to the blocks, and we can see that the target points are the centers of the blocks for the quadrotors. During the quadcopter's flight from the take-off point to the block, if there is no collision risk with other quadcopters, it will approach the block along a straight line. If there is a collision risk with other quadcopters and the current quadcopter has a lower priority, it will firstly avoid the quadcopter with collision risk, and then fly towards the block along a straight line until it reaches the block. Specifically, when the 1st quadrotor with a priority of 1 encounters the 13th quadrotor with a priority of 2, the 1st quadrotor takes avoidance action and returns to the straight-line after the 13th quadrotor leaves. The same happened when the 2nd quadrotor met the 12th quadrotor.

(3) Comparative Cooperative Test

Fig. 9 depicts the final simulation result of pesticide spraying operation with cooperative quadcopters on the block using the average and optimal mission assignment. As shown in Fig. 9, the block in the simulation test is not a standard rectangle but a right trapezoid. The vertices of the polygon block are inputted as (0, 0), (0, 100), (100, 100) and (120, 0), respectively. More specifically, the height of the block is 100 m, the length of short parallel side is 100 m, and the length of long parallel side is 120 m. The number of quadcopters m is 3, the pesticide spraying width w_0 is 6 m, and the flight altitude h is 3 m as commonly used in the pesticide spraying missions. For simplicity, three quadrotors take off and land from the same base in the simulation test. So, the number of spraying missions $n = l_r / w_0 = 20$. The average speed of quadcopters is 2 m/s. Two different simulations are carried out to verify the reasonability and correctness of the optimal mission assignment scheme. The first one is to divide all the tasks equally without optimization, whereas the second one is to adopt the proposed optimal mission assignment scheme to allocate the missions. The total time spent on the two simulations is recorded.

In order to make the experimental results more convincing, two sets of comparative experiments are carried out: one with the same number of quadrotors $m = 3$ and different block sizes, and the other with different number of quadrotors $m = 3, 4, 5, 6$ and different block sizes. The results of experiments are shown in Tables 5 and 6.

As listed in Table 5, S_{ave} and S_{opt} are the average scheme and optimal scheme, respectively, t_{ave} and t_{opt} are the spraying time based on the average scheme and optimal scheme, respectively, and t_{sav} and p_{sav} are the saving time and its percentage of the optimal scheme versus average scheme, respectively. Here, average scheme means that the paths number are divided equally regardless of block shape while the optimal scheme means that the paths number are divided by the SQP algorithm considering the shape of the block. In Scenario 1: all the number of quadrotors is 3 but the block size is different; if the numbers of spraying paths are 30, 40 and 50, the optimal scheme saves 112.4 sec, 76.0 sec, and 138.8 sec than the average scheme, which account for about 11.4%, 6.8%, and 12.5% of the spraying time based on the average scheme, respectively. As listed in Table 6, in Scenario 2: both the number of quadrotors and the field size are different; if the numbers of quadrotors are 3, 4, 5 and 6, and the numbers of paths to be sprayed are 30, 40, 50 and 60, the optimal scheme saves 112.4 sec, 194.1 sec, 260.3 sec, and 34.3 sec than the average scheme, which account for about 11.4%, 24.7%, 30.3% and 4.7% of spraying time based on the average scheme, respectively.

In Fig. 9, three quadrotors are allocated into three separate sub-blocks for operations during the spraying flight, so there is no risk for them to collide with each other during the spraying flight. Three quadcopters are assigned with 7, 7, and 6 paths by the average algorithm but assigned with 6, 6, and 8 paths by the optimal algorithm, respectively. The third quadcopter is assigned with the maximum number of paths since the block is a right trapezoid. The overall time spent on spraying pesticides based on average and optimal allocating strategy is 565.2 sec and 504.4 sec respectively, as listed in Table 7. As shown in

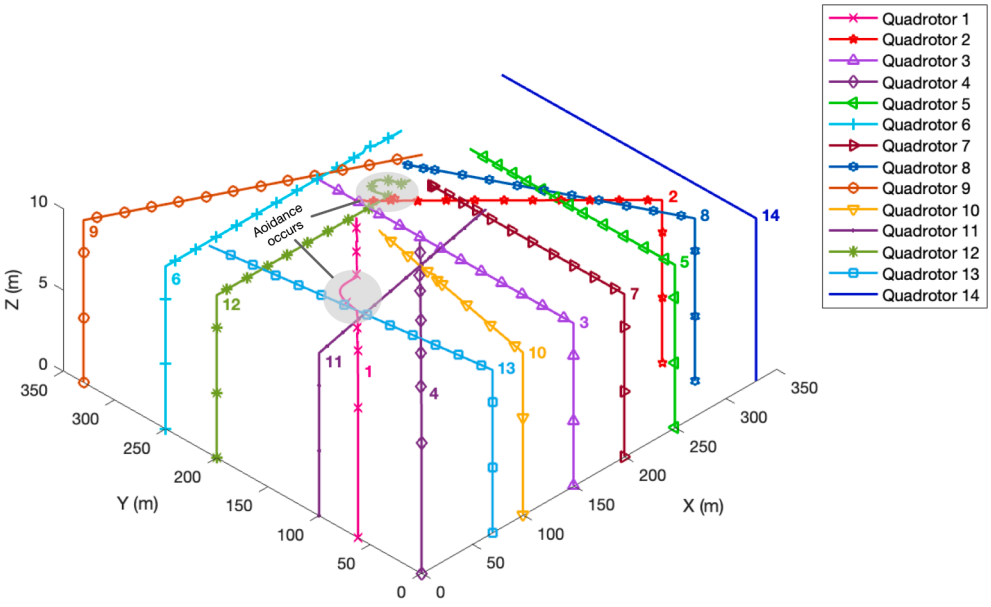

Fig. 8. The collision avoidance diagram for multiple quadrotors from the take-off point to the blocks.

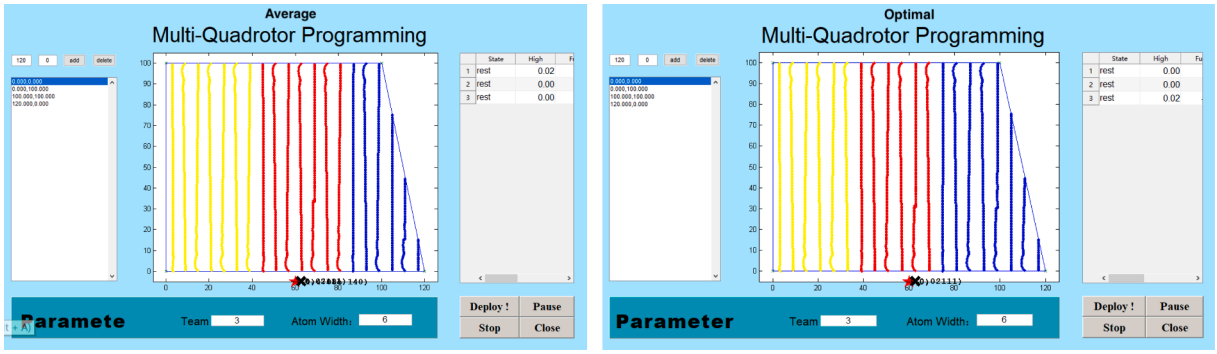

Fig. 9. The simulation results of cooperative quadcopters' spraying pesticides on the block by average and optimal mission assignments.

Table 5
Scenario 1: Results of experiments with the same number of quadrotors $m = 3$ and different field sizes.

m	n	S_{ave}	S_{opt}	t_{ave}	t_{opt}	t_{sav}	p_{sav}
3	30	10:10:10	9:12:9	985	872.6	112.4	11.4%
3	40	14:13:13	11:18:11	1116.9	1040.9	76.0	6.8%
3	50	17:17:16	15:20:15	1110.7	971.9	138.8	12.5%

Fig. 9, fewer paths are allocated to the third quadcopter, so the average allocation strategy is not reasonable. However, more paths are allocated to the third quadcopter by the optimal scheme, so the length of paths assigned to the three quadcopters is almost the same. As a result, the spraying time of three quadcopters are nearly identical. Therefore, the time spent on spraying pesticides via the optimal algorithm is shorter than that via the average algorithm. The optimal algorithm is more efficient than the average algorithm.

Therefore, regardless of Scenario 1 or Scenario 2, the optimal scheme proposed in this paper can effectively save the time to complete all the spraying tasks, which also proves the rationality and correctness of the optimal task allocation algorithm proposed in this paper.

6.2. Real flight tests

Fig. 10 shows the ZY-UAV-680 quadcopter frame produced by the industrial partner China Beijing Droneyee Intelligent Technology Co., Ltd. as the test platform, and it supports the MATLAB/Simulink model-based design by open-source system Pixhawk 2.4.8. It is easy to download flight data from this open-source system for further analysis and comparison. Although the plant protection UAVs are customized to pesticide spraying tasks, these industrial UAVs are not open source to general users, and the flight data cannot be downloaded for analysis and comparison. The dimensions of the quadcopter are 870 mm × 870 mm × 420 mm, and the airframe weighs 3,524 g. The frame of whole quadcopter is constructed with carbon fiber. The carried Ace High Discharge LI-PO battery with a capacity of 16,000 mAh can help it fly for more than 15 min. Its hovering accuracy under the positioning system can reach ± 0.15 m. The maximum vertical speed of the quadcopter is 2 m/s, while the maximum horizontal flight speed can reach 15 m/s.

To compare the two algorithms proposed in this paper, a real simulating flight test is conducted by these quadcopters. Since the constraints on test ground and communication distance is limited, we adopt a scaled method which shrinks the size of block being half of the simulation. In this scaled method, the shorter base, longer base, and height of the block in the actual flight test are set to be half of those involved in the simulated block in Fig. 9, which are 50 m, 60 m, and 50 m, respectively, as listed in Table 7. The average speed V and the pesticide spraying width w_0 are also half of the simulated parameters, which are 1 m/s and 3 m, respectively. The flight altitude is set to about 10 m according to the following reasons: first, the quadrotors with Pixhawk system must fly with enough altitude to keep safety. If there are occurrences of some faults or failures or the quadcopters do not follow the planned path, there are enough altitude and time for the remote pilots to control the quadcopters and land them manually with safety. In Fig. 11, there is a factory about 3 m high in the test ground, so the quadrotors must fly higher to avoid collisions. Then, in this paper, we focus on the missions scheduling and path planning, and do not consider the detailed pesticide spraying process. The spraying flight altitude only affects the time spent on vertical taking off and landing, and therefore it has very little impact on the final test results. The following Table 8 shows the comparative parameters of the simulation tests and the actual flight tests. The scaled method ensures that the simulation and actual tests have the same number of paths and the same spraying time spent simultaneously on each path. Therefore, the real flight tests can fit in the actual circumstance.

Fig. 11 shows the comparative real flight test video snapshot of pesticide spraying operation of multiple cooperative quadcopters on the block. The real flight test video can be watched at the link: https://www.

Table 6
Scenario 2: Results of experiments with the different number of quadrotors $m = 3, 4, 5, 6$ and different field sizes.

m	n	S_{ave}	S_{opt}	t_{ave}	t_{opt}	t_{sav}	p_{sav}
3	30	10:10:10	9:12:9	985	872.6	112.4	11.4%
4	40	10:10:10:10	8:12:12:8	786.5	592.4	194.1	24.7%
5	50	10:10:10:10:10	7:11:14:11:7	858.9	598.6	260.3	30.3%
6	60	10:10:10:10:10:10	6:11:13:13:11:6	723.5	689.2	34.3	4.7%

Table 7
The comparative parameters of simulation and real flight test.

Test scheme	Shorter base, longer base, height (m)	Average speed (m)	Spraying altitude (m)	Spraying width (m)
Simulation	100, 120, 100	2	3	6
Real Flight	50, 60, 50	1	10	3

Fig. 10. ZY-UAV-680 quadcopter UAV by Droneyee Intelligent Technology Co., Ltd.

bilibili.com/video/BV1Yh411b7Hf/. One of the six separate videos describes the real flight situation of a quadcopter, and each one involves important information such as attitude, altitude, ground speed, and real-time flight path. The orange-yellow line represents the allocated paths, while the red line represents the real flight paths. The charging/refueling time of the two tests is simulated by letting the quadcopter hover at the take-off point for 17 sec. The quadcopters in both average and optimal mission assignments can follow the paths allocated by the algorithms well. However, judging from the videos proposed, it is evident that the real flight situation can fit into the real-time flight quite well.

By the average mission assignment scheme, the first and second quadcopters are both allocated 7 paths, while the third quadcopter is allocated 6 paths. In comparison, the first, second, and third quadcopters are allocated 6, 6, and 8 paths using the optimal algorithm, respectively. The third quadcopter is assigned with the maximum number of paths.

Fig. 12 depicts the actual flight test results of pesticide spraying operation of cooperative quadcopters on the block by average and optimal mission assignments. Three quadrotors may collide with each other during the take-off process or the landing process if they finish the operations almost at the same time. In Fig. 12, the take-off and landing spots (bases) of the quadrotors are set a safe distance away from each other, so they can take off and land safely without colliding with each other. Although the bases of three quadrotors are different in the average scheme and optimal scheme, the distances from the bases to the block are almost the same. In Table 8, the time spent on the three paths by the average scheme are 525 sec, 605 sec, and 405 sec, respectively. Therefore, the overall time is 605 sec. In comparison, the time spent on the three paths by the optimal scheme are 411 sec, 495 sec, and 525 sec, respectively. So, the overall flight time is 525 sec. Since the spraying flight altitude of real tests are higher than that of simulations, the real tests spend more time than simulation during the taking off and landing process, and finally the real tests spend a little more time than simulation during the total tests. The time differences between the simulation test and real flight test of average scheme and optimal scheme are 39.8 sec and 20.6 sec, which account for 6.6% and 3.9% of the time spent on the real flight test, respectively. The optimal algorithm can save 60.8 sec and 80 sec in the simulation test and the real flight test, which account for 10.8% and 13.2% of the time spent on the average scheme, respectively. It can be concluded that the real fight test matches the simulation result, and the optimal algorithm is more efficient than the average algorithm.

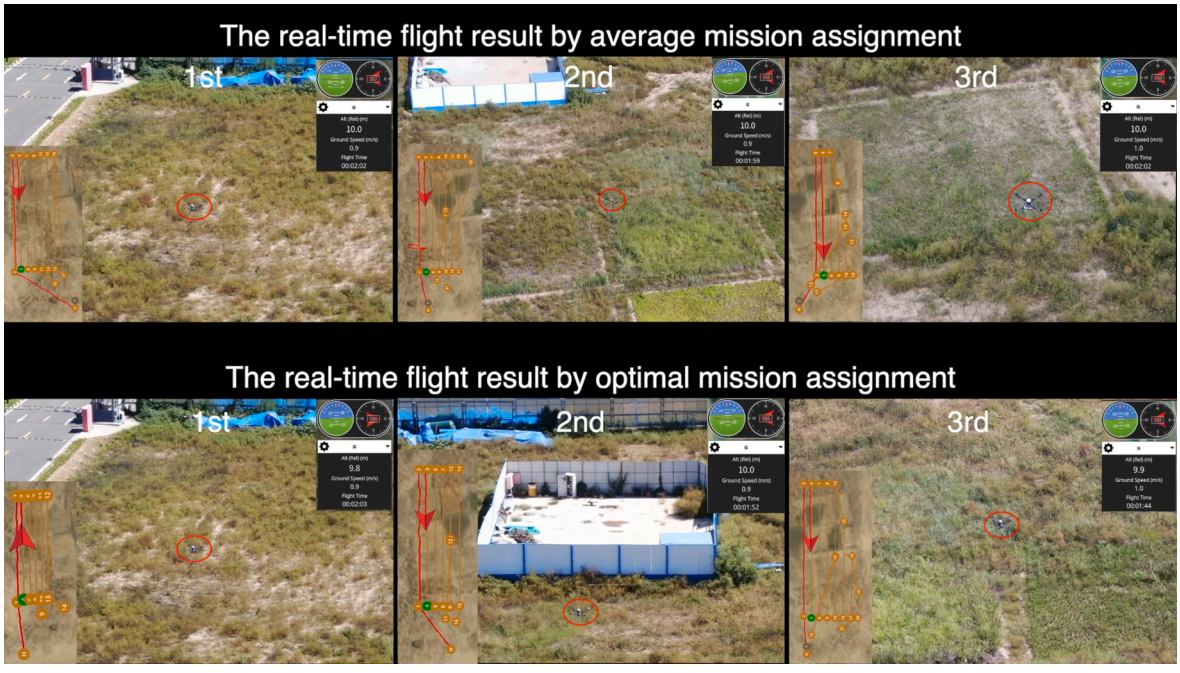

Fig. 11. The comparative actual flight test video snapshots of pesticide spraying operation of cooperative quadcopters on the block.

Table 8
The simulation and real flight test results of three quadrotors by two comparative algorithms.

Assignment scheme	Allocation scheme	Allocation time (sec)	Simulation time (sec)	Real flight Time (sec)	Time difference (sec)	Time difference (%)
Average	7:7:6	525:605:405	565.2	605	39.8	6.6%
Optimal	6:6:8	411:495:525	504.4	525	20.6	3.9%

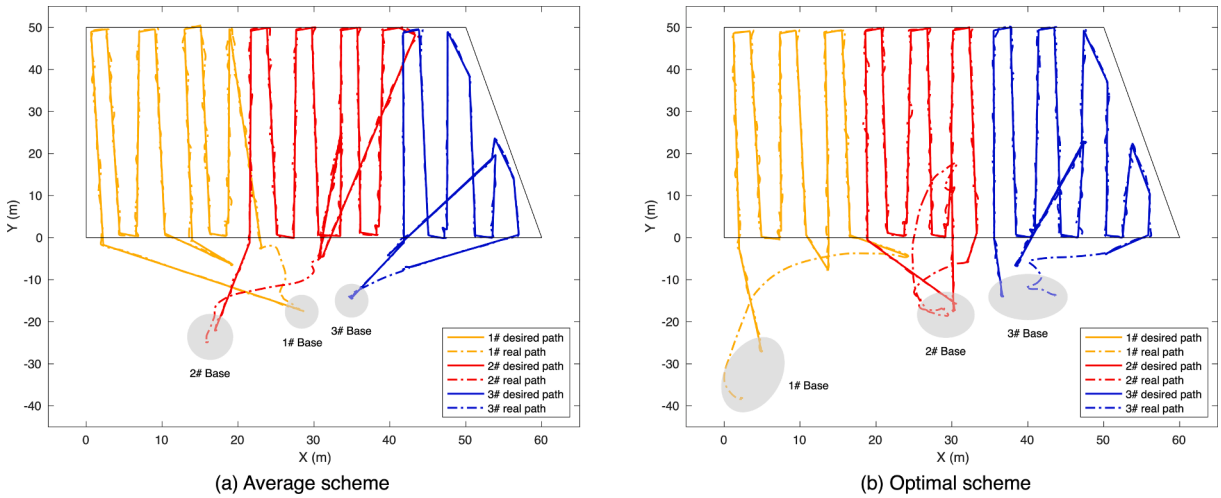

Fig. 12. The actual flight test results of pesticide spraying operation of cooperative quadcopters on the block by average and optimal mission assignment.

6.3. Discussion and analysis

Li et al. (2022) compared Order Irrelevant Enumeration Solution (OIES), Equal Task Assignment (ETA), Sequential Task Assignment (STA), Discrete Particle Swarm Optimization (DPSO), and full permutation algorithm for CPP task of multiple crop protection UAVs. The ETA strategy corresponds to the average strategy in this paper. Li et al. (2022) aimed to allocate the UAVs of a known number to a block. In our research work, we consider in advance that how should multiple quadcopters be divided reasonably for several blocks. To guarantee the whole minimum spraying time, the dividing strategy should ensure that more quadcopters should be allocated to blocks either far away from the take-off point or with more spraying tasks, while fewer quadcopters should be allocated to blocks either closer to the take-off point or with fewer spraying tasks.

After conducting the task assignment test, we continued to carry out the comparative test by cooperative UAVs. To compare the efficiency of different allocating strategies, two categories of experiments are implemented: one with the same number of quadrotors $m = 3$ but different block sizes, and the other with different numbers of quadrotors $m = 3, 4, 5, 6$ and different block sizes. Both two sets of experiments show that the optimal strategy can save spraying time, making it more efficient.

Limited by the experimental conditions, three cooperative quadrotors are employed in the actual flight tests to verify the optimal algorithm in this paper. The shorter base, longer base, and height of the real blocks are set to be half those involved in the simulated blocks, and the average speed and the pesticide spraying width are also half the simulated parameters. As a result, this scaled method ensures that the simulation and actual tests have the same overall spraying time. The comparative results between the simulation test and actual test suggest that the real flight test matches the simulation, and the optimal strategy is also more efficient than the average strategy.

7. Conclusions and future works

This paper has proposed an autonomous task assignment and decision-making algorithm for multiple pesticide spraying quadcopters. Firstly, the mathematical model of pesticide spraying by multiple cooperative quadcopters is established, and SQP by the state machine is adopted as the optimization method to solve the proposed problem. Then, the air traffic scheduling system and user's demands, including the functional and safety demands are introduced to define the flight modes. Finally, the simulation platform by MATLAB GUIs and Stateflow is established. The simulation and the actual flight test by Droneyee ZY-UAV-680 quadcopters are carried out. Both test cases show that the simulation result can match the real flight test well, and the optimal algorithm is more efficient than the average algorithm. In future studies, the proposed algorithm for coverage path planning will be promoted and improved in three-dimensional space by the established simulation platform in this work.

CRediT authorship contribution statement

Jing Huang: Data curation, Formal analysis, Funding acquisition, Investigation, Methodology, Project administration, Writing – original draft, Writing – review & editing, Project administration. **Yao Luo:** Data curation, Investigation, Methodology, Software, Writing – original draft. **Quan Quan:** Conceptualization, Formal analysis, Supervision, Project administration, Writing – review & editing. **Ban Wang:** Funding acquisition, Writing – review & editing. **Xianghong Xue:** Formal analysis, Writing – review & editing. **Youmin Zhang:** Funding acquisition, Supervision, Project administration, Writing – review & editing.

Declaration of Competing Interest

The authors declare that they have no known competing financial interests or personal relationships that could have appeared to influence the work reported in this paper.

Data availability

Data will be made available on request.

Acknowledgments

This work is supported in part by the National Natural Science Foundation of China (61833013, 62003266, and 62103326), the Science and Technology Department of Jiangxi Province (20192BBEL50005), the China Postdoctoral Science Foundation (2021MD703880), and the Natural Sciences and Engineering Research Council of Canada.

Sincere gratitude should be extended to Droneyee Intelligent Technology Co., Ltd. for providing UAVs, experimental flight test site, and technical support.

References

Choset, H., Pignon, P., 1998. Coverage path planning: The Boustrophedon cellular decomposition. In: Zelinsky, A. (Ed.), Field and Service Robotics. Springer London, London, pp. 203–209. https://doi.org/10.1007/978-1-4471-1273-0_32.

Dai, R., Fotedar, S., Radmanesh, M., Kumar, M., 2018. Quality-aware UAV coverage and path planning in geometrically complex environments. Ad Hoc Netw. 73, 95–105. https://doi.org/10.1016/j.adhoc.2018.02.008.

Du, B., 2017. A precision spraying mission assignment and path planning performed by multi-quadcopters. In: 2017 2nd International Conference on Electrical, Control and Automation Engineering (ECAE 2017). Atlantis Press, pp. 233–237.

Ellefsen, K.O., Lepikson, H.A., Albiez, J.C., 2017. Multiobjective coverage path planning: Enabling automated inspection of complex, real-world structures. Appl. Soft Comput. 61, 264–282. https://doi.org/10.1016/j.asoc.2017.07.051.

Galceran, E., Carreras, M., 2013. A survey on coverage path planning for robotics. Rob. Auton. Syst. 61, 1258–1276. https://doi.org/10.1016/j.robot.2013.09.004.

Glorieux, E., Franciosa, P., Ceglarek, D., 2020. Coverage path planning with targetted viewpoint sampling for robotic free-form surface inspection. Robot. Comput.-Integr. Manuf. 61, 101843 https://doi.org/10.1016/j.rcim.2019.101843.

Granna, J., Godage, I.S., Wirz, R., Weaver, K.D., Webster, R.J., Burgner-Kahrs, J., 2016. A 3-D volume cage path planning algorithm with application to intracerebral hemorrhage evacuation. IEEE Robot. Autom. Lett. 1, 876–883. https://doi.org/10.1109/LRA.2016.2528297.

Guastella, D.C., Cantelli, L., Giammello, G., Melita, C.D., Spatino, G., Muscato, G., 2019. Complete coverage path planning for aerial vehicle flocks deployed in outdoor environments. Comput. Electr. Eng. 75, 189–201. https://doi.org/10.1016/j.compeleceng.2019.02.024.

Han, G., Zhou, Z., Zhang, T., Wang, H., Liu, L., Peng, Y., Guizani, M., 2020. Ant-colony-based complete-coverage path-planning algorithm for underwater gliders in ocean areas with thermoclines. IEEE Trans. Veh. Technol. 69, 8959–8971. https://doi.org/10.1109/TVT.2020.2998137.

Hassan, M., Liu, D., 2020. PPCPP: A predator–prey-based approach to adaptive coverage path planning. IEEE Trans. Rob. 36, 284–301. https://doi.org/10.1109/TRO.2019.2946891.

Hassanalian, M., Abdelkefi, A., 2017. Classifications, applications, and design challenges of drones: A review. Prog. Aerosp. Sci. 91, 99–131. https://doi.org/10.1016/j.paerosci.2017.04.003.

Hossain, F.A., Zhang, Y., Yuan, C., 2019. A survey on forest fire monitoring using unmanned aerial vehicles. In: 2019 3rd International Symposium on Autonomous Systems (ISAS). IEEE, Shanghai, China, pp. 484–489. https://doi.org/10.1109/ISASS.2019.8757707.

Khuller, S., Malekian, A., Mestre, J., 2011. To fill or not to fill: The gas station problem. ACM Trans. Algorithms 7 (3), 1–16. https://doi.org/10.1145/1978782.1978791.

Li, J., Xiong, Y., She, J., Wu, M., 2020. A path planning method for sweep coverage with multiple UAVs. IEEE Internet Things J. 7, 8967–8978. https://doi.org/10.1109/JIOT.2020.2999083.

Li, Y., Xu, Y., Xue, X., Liu, X., Liu, X., 2022. Optimal spraying task assignment problem in crop protection with multi-UAV systems and its order irrelevant enumeration solution. Biosyst. Eng. 214, 177–192. https://doi.org/10.1016/j.biosystemseng.2021.12.018.

Lindner, S., Garbe, C., Mombaur, K., 2019. Optimization based multi-view coverage path planning for autonomous structure from motion recordings. IEEE Robot. Autom. Lett. 4, 3278–3285. https://doi.org/10.1109/LRA.2019.2926216.

Macleod, C.N., Dobie, G., Pierce, S.G., Summan, R., Morozov, M., 2018. Machining-based coverage path planning for automated structural inspection. IEEE Trans. Autom. Sci. Eng. 15, 202–213. https://doi.org/10.1109/TASE.2016.2601880.

Mansouri, S.S., Kanellakis, C., Fresk, E., Kominiak, D., Nikolakopoulos, G., 2018a. Cooperative coverage path planning for visual inspection. Control Eng. Pract. 74, 118–131. https://doi.org/10.1016/j.conengprac.2018.03.002.

Mansouri, S.S., Kanellakis, C., Georgoulas, G., Kominiak, D., Gustafsson, T., Nikolakopoulos, G., 2018b. 2D visual area coverage and path planning coupled with camera footprints. Control Eng. Pract. 75, 1–16. https://doi.org/10.1016/j.conengprac.2018.03.011.

Mukherjee, A., Misra, S., Raghuwanshi, N.S., 2019. A survey of unmanned aerial sensing solutions in precision agriculture. J. Netw. Comput. Appl. 148, 102461 https://doi.org/10.1016/j.jnca.2019.102461.

Nasr, S., Mekki, H., Bouallegue, K., 2019. A multi-scroll chaotic system for a higher coverage path planning of a mobile robot using flatness controller. Chaos Solitons Fractals 118, 366–375. https://doi.org/10.1016/j.chaos.2018.12.002.

Nilsson, R.S., Zhou, K., 2020. Method and bench-marking framework for coverage path planning in arable farming. Biosyst. Eng. 198, 248–265. https://doi.org/10.1016/j.biosystemseng.2020.08.007.

Quan, Q., 2017. Introduction to multicopter design and control (pp. 150-160). Singapore: Springer. https://doi.org/10.1007/978-981-10-3382-7.

Quan, Q., Dai, X., Wang, S., 2020. Multicopter design and control practice: A series experiments based on MATLAB and Pixhawk. Springer: Singapore. https://doi.org/10.1007/978-981-15-3138-5.

Sandamurthy, K., Ramanujam, K., 2020. A hybrid weed optimized coverage path planning technique for autonomous harvesting in cashew orchards. Inf. Process. Agric. 7, 152–164. https://doi.org/10.1016/j.inpa.2019.04.002.

Shi, L., Xu, S., Liu, H., Zhan, Z., 2020. QoS-aware UAV coverage path planning in 5G mmWave network. Comput. Netw. 175, 107207 https://doi.org/10.1016/j.comnet.2020.107207.

Silveira, F., Lermen, F.H., Amaral, F.G., 2021. An overview of Agriculture 4.0 development: Systematic review of descriptions, technologies, barriers, advantages, and disadvantages. Comput. Electron. Agric. 189, 106405 https://doi.org/10.1016/j.compag.2021.106405.

Sinha, J., 2020. Aerial robot for smart farming and enhancing farmers' net benefit. Indian J. Agric. Sci. 90, 258–267.

Su, J., Liu, C., Coombes, M., Hu, X., Wang, C., Xu, X., Li, Q., Guo, L., Chen, W.-H., 2018. Wheat yellow rust monitoring by learning from multispectral UAV aerial imagery. Comput. Electron. Agric. 155, 157–166. https://doi.org/10.1016/j.compag.2018.10.017.

Sun, B., Zhu, D., Tian, C., Luo, C., 2019. Complete coverage autonomous underwater vehicles path planning based on Glasius bio-inspired neural network algorithm for discrete and centralized programming. IEEE Trans. Cogn. Dev. Syst. 11, 73–84. https://doi.org/10.1109/TCDS.2018.2810235.

Sundar, K., Rathinam, S., 2014. Algorithms for routing an unmanned aerial vehicle in the presence of refueling depots. IEEE Trans. Autom. Sci. Eng. 11, 287–294. https://doi.org/10.1109/TASE.2013.2279544.

Torres, M., Pelta, D.A., Verdegay, J.L., Torres, J.C., 2016. Coverage path planning with unmanned aerial vehicles for 3D terrain reconstruction. Expert Syst. Appl. 55, 441–451. https://doi.org/10.1016/j.eswa.2016.02.007.

Vinh, K., Gebreyohannes, S., Karimoddini, A., 2019. An area-decomposition based approach for cooperative tasking and coordination of uavs in a search and coverage mission. In: 2019 IEEE Aerospace Conference. IEEE, pp. 1–8. https://doi.org/10.1109/AERO.2019.8741565.

Wang, L., Xu, M., Hou, Q., Wang, Z., Lan, Y., Wang, S., 2021. Numerical verification on influence of multi-feature parameters to the downwash airflow field and operation effect of a six-rotor agricultural UAV in flight. Comput. Electron. Agric. 190, 106425 https://doi.org/10.1016/j.compag.2021.106425.

Xu, Y., Xue, X., Sun, Z., Chang, C., Gu, W., Chen, C., Jin, Y., Peng, B., 2019. Online spraying quality assessment system of plant protection unmanned aerial vehicle based on Android client. Comput. Electron. Agric. 166, 104938 https://doi.org/10.1016/j.compag.2019.104938.

Yang, X., Shu, L., Chen, J., Ferrag, M.A., Wu, J., Nurellari, E., Huang, K., 2021. A survey on smart agriculture: Development modes, technologies, and security and privacy challenges. IEEE/CAA J. Autom. Sin. 8, 273–302. https://doi.org/10.1109/JAS.2020.1003536.

Yao, L., Jiang, Y., Zhiyao, Z., Shuaishuai, Y., Quan, Q., 2016. A pesticide spraying mission assignment performed by multi-quadcopters and its simulation platform establishment. In: 2016 IEEE Chinese Guidance, Navigation and Control Conference (CGNCC). IEEE, Nanjing, China, pp. 1980–1985. https://doi.org/10.1109/CGNCC.2016.7829093.

Yuan, C., Zhang, Y., Liu, Z., 2015. A survey on technologies for automatic forest fire monitoring, detection, and fighting using unmanned aerial vehicles and remote sensing techniques. Can. J. For. Res. 45, 783–792. https://doi.org/10.1139/cjfr-2014-0347.

Zhou, Y., Zhao, H., Liu, Y., 2020. An evaluative review of the VTOL technologies for unmanned and manned aerial vehicles. Comput. Commun. 149, 356–369. https://doi.org/10.1016/j.comcom.2019.10.016.

Zuo, Z., Liu, C., Han, Q.-L., Song, J., 2022. Unmanned aerial vehicles: Control methods and future challenges. IEEE/CAA J. Autom. Sin. 9, 601–614. https://doi.org/10.1109/JAS.2022.105410.